A New Approach for Simultaneous AVR-PSS Design

Bevrani H.

Published (to be published) in: Technical report, University of Kurdistan, Sanandaj, Iran,

(Expected) publication date: 2007

گزارش نهایی طرح پژوهشی

دانشکدهٔ مهندسی

گروه مهندسی برق

عنوان طرح:

روشی نو برای طراحی همزمان
تنظیم‌کننده‌های خودکار ولتاژ و پایدارساز دینامیکی سیستمهای قدرت

مجری: **حسن بیورانی**

همکار: **تاکاشی هیاما**

تاریخ تصویب: ۸۵/۹/۱۸

تاریخ خاتمه: ۸٦/٤/۲۳

دانشگاه کردستان
دانشکده مهندسی
گروه مهندسی برق

روشی نو برای طراحی همزمان تنظیم‌کننده‌های خودکار ولتاژ و پایدارساز دینامیکی در سیستم‌های قدرت

مجری: حسن بیورانی
همکار: تاکاشی هیاما

تیرماه ۱۳۸۶

FINAL REPORT OF RESEARCH PROJECT

Faculty of Engineering

Department of Electrical Engineering

Title:

A New Approach for Simultaneous AVR-PSS Design

By: **Hassan Bevrani**

Co-Author: **Takashi Hiyama**

Approval Date: **December 9, 2006**

Complement Date: **July 15, 2007**

University of Kurdistan
Faculty of Engineering
Department of Electrical Engineering

A New Approach for Simultaneous AVR-PSS Design

Author:
Hassan Bevrani

Co-Author:
Takashi Hiyama

July 2007

Abstract

This paper addresses a control methodology to enhance power system dynamic stability and voltage regulation by augmenting existing generator controls (conventional PSS and AVR) using an optimal static gain vector. The control design problem is reduced to find a new control loop including a simple fixed gain vector. In order to optimal tuning of gain elements, the problem is formulated via an H∞ static output feedback (H∞-SOF) control technique, and the solution is easily carried out using an iterative linear matrix inequalities (ILMI) algorithm.

It is shown that we can easily remove the conventional PSS and AVR and replace those by the mentioned simple H∞-SOF controller. Real-time experiment has been performed for a longitudinal four-machine infinite-bus system on the Analog Power System Simulator at the Research Laboratory of the Kyushu Electric Power Co*. The proposed robust technique is shown to maintain the robust performance and minimize the effects of disturbances.

Keywords:
Power system stabilizer, voltage regulation, H∞ control, static output feedback, LMI.

* Fukuoka, Japan

CONTENTS

1. Introduction

Power systems continuously experience changes in operating conditions due to variations in generation/load and a wide range of disturbances. Power system stability and voltage regulation have been considered as an important problem for secure system operation over the years (Kundur et al., 2004). Currently, because of expanding physical setups, functionality and complexity of power systems, the mentioned problem becomes a more significant than the past. That is why in recent years a great deal of attention has been paid to application of advanced control techniques in power system as one of the more promising application areas.

Conventionally, the automatic voltage regulation and power system stabilizer (AVR-PSS) design is considered as a sequential design including two separate stages. Firstly, the AVR is designed to meet the specified voltage regulation performance and then the PSS is designed to satisfy the stability and required damping performance. It is known that the stability and voltage regulation are ascribed to different model descriptions, and it has been long recognized that AVR and PSS have inherent conflicting objectives (Law, Hill & Godfrey, 1994; Law et al., 1994; Venikov & Stroev, 1971).

In the last two decades, some studies have considered an integrated design approach to AVR and PSS design using domain partitioning (Venikov & Stroev, 1971), robust pole-replacement (Soliman & Sakar, 1988) and adaptive control (Malik et al., 1986). Moreover, recently several control methods have been made to coordinate the various requirements for stabilization and voltage regulation within the one new control structure (Heniche et al., 1995; Wang & Hill, 1996; Guo et al. 2001; Yadaiah, Kumar & Bhattacharya, 2004; Bevrani & Hiyama, 2006).

Although most of addressed approaches have been proposed based on new contributions in modern control systems, because of following two main reasons, they are not well suited to meet the design objectives in a real multi-machine power system: *i*) The complexity of control structure, numerous unknown design parameters and neglecting real constraints can be frequently seen in the most of new suggested techniques. While in real world power systems, usually controllers with simple structure are desirable. That is why electric industry still uses the simple PI, PID and Lead-lag controllers that their parameters are commonly tuned based on classical, experiences and trial-and-error approaches. *ii*) Experiences show although the conventional PSS and AVR systems are incapable to obtain good dynamical performance for a wide range of operating conditions and disturbances, the real electric industry because of some probable risks, bugs and/or having a complex structure is too conservative to open the conventional control loops and test the novel/advanced controllers.

In response to above problems, this paper presents a methodology to enhance the stability and voltage regulation of existing real power system with and without their conventional PSS and AVR devices. The methodology provides a simple gain vector in parallel with the conventional control devices. The design objectives are formulated via an H∞-SOF control problem and the optimal static gains are obtained using an ILMI algorithm. The preliminary step of this work has been presented in (Bevrani & Hiyama, 2006).

The proposed controller in the present paper uses the measurable signals and has merely proportional gains; so gives considerable promise for implementation, especially in a multi-machine system. In fact the proposed control strategy attempts to make a bridge between the simplicity of control structure and robustness of stability and performance to satisfy the simultaneous AVR and PSS tasks.

To demonstrate the efficiency of the proposed control method, some real time nonlinear laboratory tests have been performed on a four-machine infinite-bus system using the large scale Analog Power System Simulator at the Research Laboratory of the Kyushu Electric Power Company (Japan). The obtained results are compared with a conventional AVR-PSS system.

2. Proposed Control Strategy

2.1. A Background on H∞-SOF Control Design

This section gives a brief overview for the H∞-SOF control design. Consider a linear time invariant system $G(s)$ with the following state-space realization.

$$G_i(s):\begin{aligned}\dot{x}_i &= A_i x_i + B_{1i} w_i + B_{2i} u_i \\ z_i &= C_{1i} x_i + D_{12i} u_i \\ y_i &= C_{2i} x_i\end{aligned} \tag{1}$$

where x_i is the state variable vector, w_i is the disturbance and area interface vector, z_i is the controlled output vector and y_i is the measured output vector. The A_i, B_{1i}, B_{2i}, C_{1i}, C_{2i} and D_{12i} are known real matrices of appropriate dimensions.

The H∞-SOF control problem for the linear time invariant system $G_i(s)$ with the state-space realization of (1) is to find a gain matrix K_i ($u_i = K_i y_i$), such that the resulted closed-loop system is internally stable, and the H∞ norm from w_i to z_i (Fig. 1) is smaller than γ, a specified positive number, i.e.

$$\left\| T_{z_i w_i}(s) \right\|_\infty < \gamma \tag{2}$$

It is notable that the H∞-SOF control problem can be transferred to a generalized SOF stabilization problem which is expressed via the following theorem (Cao et al., 1998).

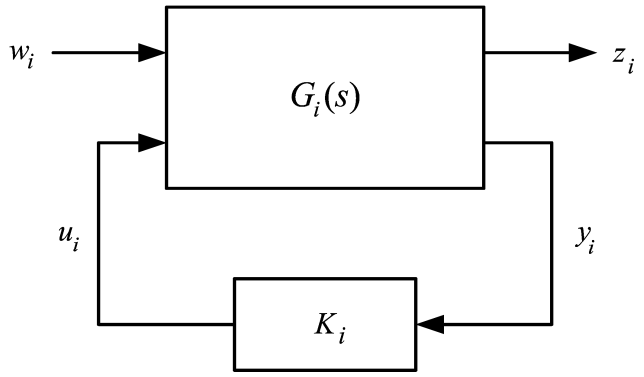

Fig. 1. Closed-loop system via H∞-SOF control.

Theorem. The system (*A, B, C*) is stabilizable via SOF if and only if there exist $P>0$, $X>0$ and K_i satisfying the following quadratic matrix inequality

$$\begin{bmatrix} A^T X + XA - PBB^T X - XBB^T P + PBB^T P & (B^T X + K_i C)^T \\ B^T X + K_i C & -I \end{bmatrix} < 0 \tag{3}$$

Here, the matrices A, B and C are constant and have appropriate dimensions. The X and P are symmetric and positive-definite matrices.

Since a solution for the consequent non convex optimization problem (3) can not be directly achieved by using general LMI technique (Boyd et al., 1994), a variety of methods were proposed by many researchers with many analytical and numerical methods to approach a local/global solution. In this paper, to solve the resulted SOF problem, an iterative LMI is used based on the existence necessary and sufficient condition for SOF stabilization, via the H∞ control technique.

2.2. Modeling

In order to design a robust power system controller, it is first necessary to consider an appropriate linear mathematical description of multi-machine power system with two axis generator models. In the view point of "generator unit *i*", the state space representation model for such a system has the form

$$\begin{aligned} \dot{x}_{1gi} &= x_{2gi} \\ \dot{x}_{2gi} &= -(D_i/M_i)x_{2gi} - (1/M_i)\Delta P_{ei}(x) \\ \dot{x}_{3gi} &= -(1/T'_{d0i})x_{3gi} - (\Delta x_{di}(x)/T'_{d0i})\Delta I_{di}(x) + u_{gi} \\ \dot{x}_{4gi} &= -(1/T'_{q0i})x_{4gi} - (\Delta x_{qi}(x)/T'_{q0i})\Delta I_{qi}(x) \end{aligned} \tag{4}$$

where the states

$$x_{gi}^T = \begin{bmatrix} x_{1gi} & x_{2gi} & x_{3gi} & x_{4gi} \end{bmatrix} = \begin{bmatrix} \delta_i & \omega_i & E'_{qi} & E'_{di} \end{bmatrix} \tag{5}$$

are defined as deviation form the equilibrium values

$$x_{egi}^T = \begin{bmatrix} \delta_{1i}^e & \omega_{2i}^e & E'^e_{qi} & E'^e_{di} \end{bmatrix}$$

and, here

$$\Delta x_{di} = x_{di} - x'_{di}\,,\ \Delta x_{qi} = x_{qi} - x'_{di} \tag{6}$$

$$\Delta P_{ei}(x) = (E'_{di} I_{di} + E'_{qi} I_{qi}) - (E'^e_{di} I^e_{di} + E'^e_{qi} I^e_{qi}) \tag{7}$$

$$\begin{aligned} I_{di} = &\sum_k [G_{ik} \cos\delta_{ik} + B_{ik} \sin\delta_{ik}] E'_{dk} \\ &+ \sum_k [G_{ik} \sin\delta_{ik} - B_{ik} \cos\delta_{ik}] E'_{qk} \end{aligned} \tag{8}$$

$$I_{qi} = \sum_k [B_{ik}\cos\delta_{ik} - G_{ik}\sin\delta_{ik}]E'_{dk} + \sum_k [G_{ik}\cos\delta_{ik} + B_{ik}\sin\delta_{ik}]E'_{qk} \tag{9}$$

A detailed description of all symbols and quantities can be found in (Sauer & Pai, 1998). Using the linearization technique and after some manipulation, the nonlinear state equations (4) can be expressed in the form of following linear state space model.

$$\dot{x}_{gi} = A_{gi}x_{gi} + B_{gi}u_{gi} \tag{10}$$

where

$$A_{gi} = \begin{bmatrix} 0 & 1 & 0 & 0 \\ a_{21} & -\frac{D_i}{M_i} & a_{23} & a_{24} \\ a_{31} & 0 & a_{33} & -\frac{G_{ii}\Delta x_{di}}{T'_{d0i}} \\ a_{41} & 0 & \frac{G_{ii}\Delta x_{qi}}{T'_{q0i}} & a_{44} \end{bmatrix}, B_{gi} = \begin{bmatrix} 0 \\ 0 \\ 1 \\ \frac{1}{T'_{d0i}} \\ 0 \end{bmatrix} \tag{11}$$

with elements that are given in Appendix. Considering the conventional AVR-PSS system we can write

$$u_{gi} = u_{ci} + u_i \tag{12}$$

where, u_{ci} is the output of conventional AVR-PSS system and the u_i is the new control input (Fig. 2). Therefore, the overall system can be described as follows:

$$\dot{x}_i = A_i x_i + B_i u_i \tag{13}$$

and,

$$x_i^T = \begin{bmatrix} x_{gi_{1\times 4}} & x_{ci_{1\times m}} \end{bmatrix}_{1\times(4+m)} \tag{14}$$

Here, the x_{ci} shows the state vector of conventional AVR-PSS system and *m* represents its dynamic order.

2.3. Proposed Control Framework

The overall control structure using SOF control design for an assumed power system with and without conventional PSS-AVR is shown in Fig. 2, where blocks PSS and AVR represents the existing conventional power system stabilizer and voltage regulators. Here the electrical power signal Δp_{ei} is considered as input signal for the PSS unit. The optimal gain vector uses the terminal voltage Δv_{ti}, electrical power Δp_{ei} and machine speed $\Delta\omega_i$ as input signals. Δv_{refi} and d_i show the

reference voltage deviation and system disturbance input, respectively.

Using the linearized model for a given power system unit "*i*" in the form of (1) and performing the standard H∞-SOF configuration (Fig. 1) with considering an appropriate controlled output signals results an effective control framework, which is shown in Fig. 3. This control structure adapts the H∞-SOF control technique with the described power system control targets and allows direct trade-off between voltage regulation and closed-loop stability by merely tuning of a vector gain.

Here, disturbance input vector w_i, controlled output vector z_i and measured output vector y_i are considered as follows:

$$w_i^T = \left[\Delta v_{refi} \quad d_i\right] \tag{15}$$

$$z_i^T = [\eta_{1i}\Delta v_{ti} \quad \eta_{2i}\Delta\delta_i \quad \eta_{3i}u_i] \tag{16}$$

$$y_i^T = \left[\Delta v_{ti} \quad \Delta p_{ei} \quad \Delta\omega_i\right] \tag{17}$$

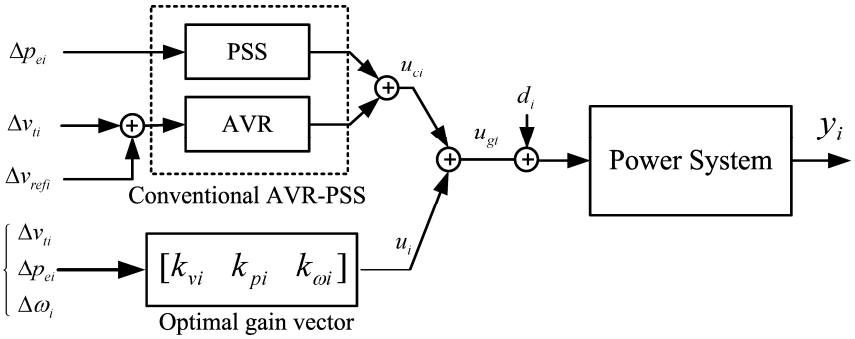

(a)

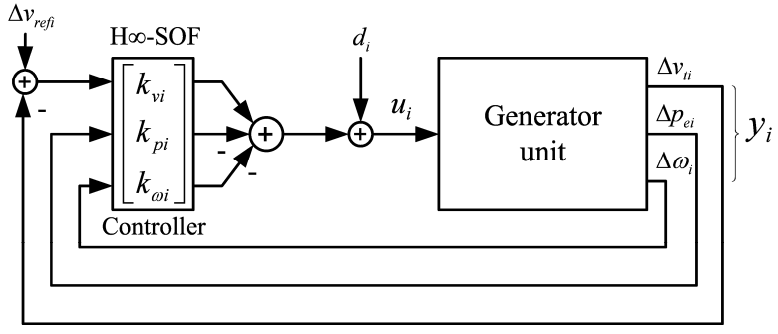

(b)

Fig. 2. Overall control structure: a) With conventional PSS-AVR; and b) Without conventional PSS-AVR

Δv_{ti} and Δp_{ei} can be easily expressed via specifies system states, and the η_{1i}, η_{2i} and η_{3i} are constant weights that must be chosen by designer to get the desired closed-loop performance. The

selection of performance constant weights η_{1i} and η_{2i} is dependent on the specified voltage regulation and damping performance goals. In fact an important issue with regard to selection of these weights is the degree to which they can guarantee the satisfaction of design performance objectives.

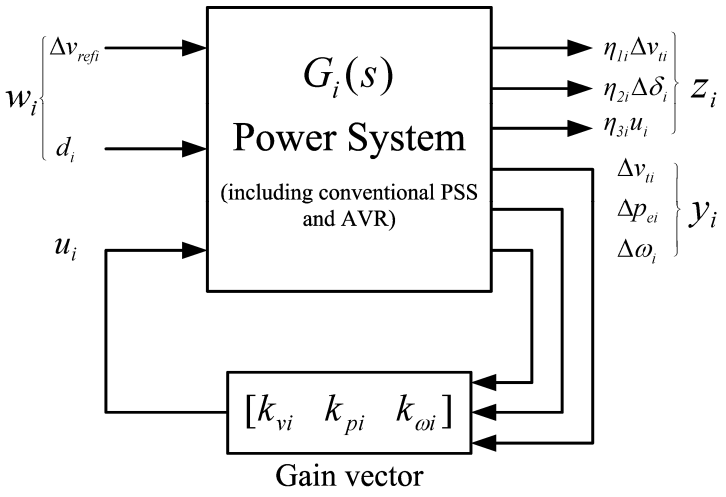

Fig. 3. The proposed H∞-SOF control framework

Furthermore, η_{3i} sets a limit on the allowed control signal to penalize fast changes, large overshoot with a reasonable control gain to meet the feasibility and the corresponded physical constraints. Since the vector z_i properly covers all significant controlled signals which must be minimized by an ideal AVR-PSS design, it is expected that the proposed robust controller could be able to satisfy the voltage regulation and stabilizing objectives, simultaneously.

The proposed control loop has the feedbacks from speed and electric power deviation signals, and, actually these two signals give the proportional-derivative (PD) information of generator speed, and acts like as phase-lead compensator in a conventional ω-type PSS. Furthermore, the additional feedback for the voltage deviation is similar to the used one in the conventional AVR (with a quite small time delay) for the measurement of voltage signal.

It is notable that, since the solution must be obtained trough the minimizing of an H∞ optimization problem, the designed feedback system satisfies the robust stability and voltage regulation performance for the overall closed-loop system. Moreover, the developed iterative LMI algorithm (which is described in the next section) provides an effective and flexible tool to find an appropriate solution in the form of a simple static gain controller.

2.4. ILMI Algorithm

It is well-known that static output feedback stabilization is still an open problem. Its reformulation generally leads to bilinear matrix inequalities (BMI) which are non-convex. This kind of problem is usually solved by an iterative algorithm that may not converge to an optimal solution.

Here, in order to solve the H∞-SOF, an iterative LMI algorithm has been used. The algorithm is mainly based on the given idea by Cao et al., 1998. The key point is to formulate the H∞ problem via a generalized static output stabilization feedback such that all eigenvalues of (A-$B\,K_i\,C$) shift

towards the left half plane in the complex s-plane, to close to feasibility of (3). The described theorem in the previous section gives a family of internally stabilizing SOF gains is defined as K_{sof}. The desirable solution K_i is an admissible SOF law

$$u_i = K_i y_i \ , \ K_i \in K_{sof} \tag{18}$$

such that

$$\left\| T_{zi\,wi}(s) \right\|_\infty < \gamma^* \ , \ \left| \gamma - \gamma^* \right| < \varepsilon \tag{19}$$

where ε is a small positive number. The performance index γ^* indicates a lower bound such that the closed-loop system is H∞ stabilizable. The optimal performance index (γ), can be obtained from the application of a full dynamic H∞ dynamic output feedback control method. The proposed algorithm, which gives an iterative LMI solution for above optimization problem includes the following steps:

Step 1. Set initial values and Compute the new system $(\overline{A}_i, \overline{B}_i, \overline{C}_i)$ for the given power system (1) as follows:

$$\overline{A}_i = \begin{bmatrix} A_i & B_{1i} & 0 \\ 0 & -\gamma I/2 & 0 \\ C_{1i} & 0 & -\gamma I/2 \end{bmatrix}, \ \overline{B}_i = \begin{bmatrix} B_{2i} \\ 0 \\ D_{12i} \end{bmatrix}, \ \overline{C}_i = \begin{bmatrix} C_{2i} & 0 & 0 \end{bmatrix} \tag{20}$$

here, $\overline{A}_i, \overline{B}_i$ and $\overline{C}_i$ are three generalized matrices.

Step 2. Set $i = 1$, $\Delta\gamma = \Delta\gamma_0$ and let $\gamma_i = \gamma_0 > \gamma$. $\Delta\gamma_0$ and γ_0 are positive real numbers.

Step 3. Select $Q > 0$, and solve $\overline{X}$ from the following algebraic Riccati equation

$$\overline{A}_i^T \overline{X} + \overline{X}\overline{A}_i - \overline{X}\overline{B}_i \overline{B}_i^T \overline{X} + Q = 0 \tag{21}$$

Set $P_1 = \overline{X}$.

Step 4. Solve the following optimization problem for $\overline{X}_i$, K_i and a_i.

Minimize a_i subject to the LMI constraints:

$$\begin{bmatrix} \overline{A}_i^T \overline{X}_i + \overline{X}_i \overline{A}_i - P_i \overline{B}_i \overline{B}_i^T \overline{X}_i - \overline{X}_i \overline{B}_i \overline{B}_i^T P_i + P_i \overline{B}_i \overline{B}_i^T P_i - a_i \overline{X}_i & (\overline{B}_i^T \overline{X}_i + K_i \overline{C}_i)^T \\ \overline{B}_i^T \overline{X}_i + K_i \overline{C} & -I \end{bmatrix} < 0 \tag{22}$$

$$\overline{X}_i = \overline{X}_i^T > 0 . \tag{23}$$

Denote a_i^* as the minimized value of a_i.

Step 5. If $a_i^* \le 0$, go to step 8.

Step 6. For $i > 1$, if $a_{i-1}^* \le 0$, $K_{i-1} \in K_{sof}$ is an H∞ controller and $\gamma^* = \gamma_i + \Delta\gamma$ indicates a lower bound such that the above system is H∞ stabilizable via SOF control. Go to step 10.

Step 7. If $i = 1$, solve the following optimization problem for $\overline{X}_i$ and K_i:

Minimize trace($\overline{X}_i$) subject to the above LMI constraints (22-23) with $a_i = a_i^*$. Denote $\overline{X}_i^*$ as the $\overline{X}_i$ that minimized trace($\overline{X}_i$).Go to step 9.

Step 8. Set $\gamma_i = \gamma_i - \Delta\gamma$, $i = i+1$. Then do steps 3 to 5.

Step 9. Set $i = i+1$ and $P_i = \overline{X}_{i-1}^*$, then go to step 4.

Step 10. If the obtained solution (K_{i-1}) satisfies the gain constraint, it is desirable, otherwise retune constant weights (η_i) and go to step 1.

The proposed iterative LMI algorithm, which is summarized in the flowchart of Fig. 4, shows that if we simply perturb $\overline{A}_i$ to $\overline{A}_i - (a/2)I$ for some $a > 0$, then we will find a solution of the matrix inequality (3) for the performed generalized plant. That is, there exist a real number ($a > 0$) and a matrix $P>0$ to satisfy inequality (22). Consequently, the closed-loop system matrix $\overline{A}_i - \overline{B}_i K \overline{C}_i$ has eigenvalues on the left-hand side of the line $\Re(s) = a$ in the complex s-plane. Based on the idea that all eigenvalues of $\overline{A}_i - \overline{B}_i K \overline{C}_i$ are shifted progressively towards the left half plane through the reduction of a. The given generalized eigenvalue minimization in the proposed iterative LMI algorithm guarantees this progressive reduction.

3. Real Time Implementation

To illustrate the effectiveness of the proposed control strategy, a real time experiment has been performed on the large scale Analog Power System Simulator at the Research Laboratory of the Kyushu Electric Power Company. For the purpose of this study, a longitudinal four-machine infinite bus system is considered as a test system. A single line representation of the study system is shown in Fig. 5. Although, in the given model the number of generators is reduced to four, it closely represents the dynamic behavior of the west part of Japan (West Japan Power System), and it is widely used by Japanese researchers (Hiyama, Oniki, Nagashima, 1996; Hiyama, Kawakita & Ono, 2004; Hiyama et al., 2005). The most important global and local oscillation modes of actual system are included. Each unit is a thermal unit, and has a separately conventional excitation control system as shown in Figs. 6a and 6b.

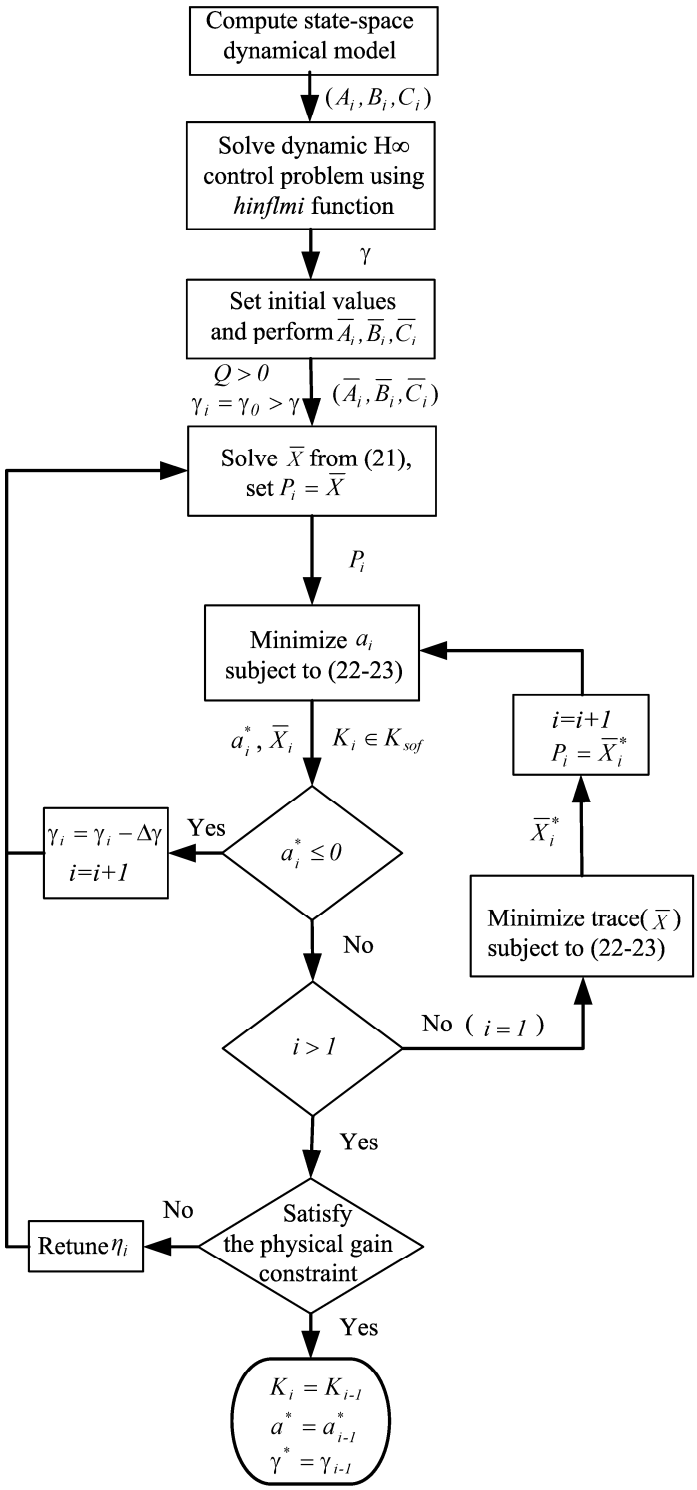

Fig. 4. Iterative LMI algorithm

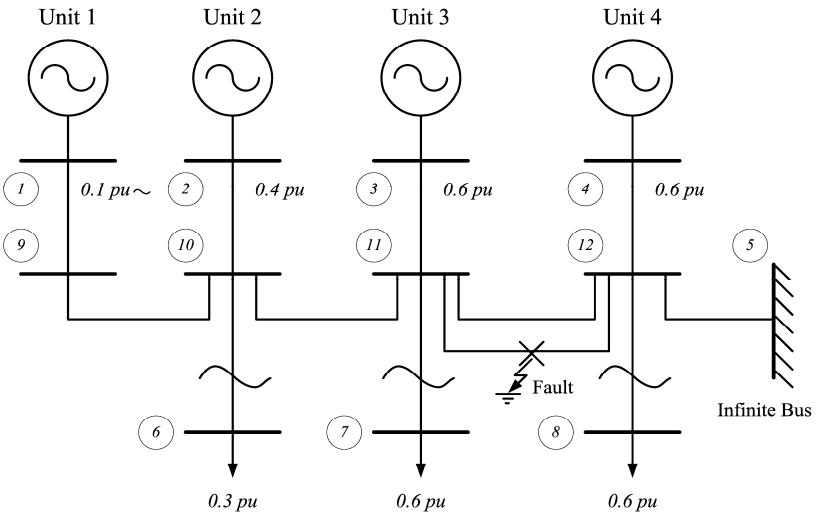

Fig. 5. Four-machine infinite-bus power system

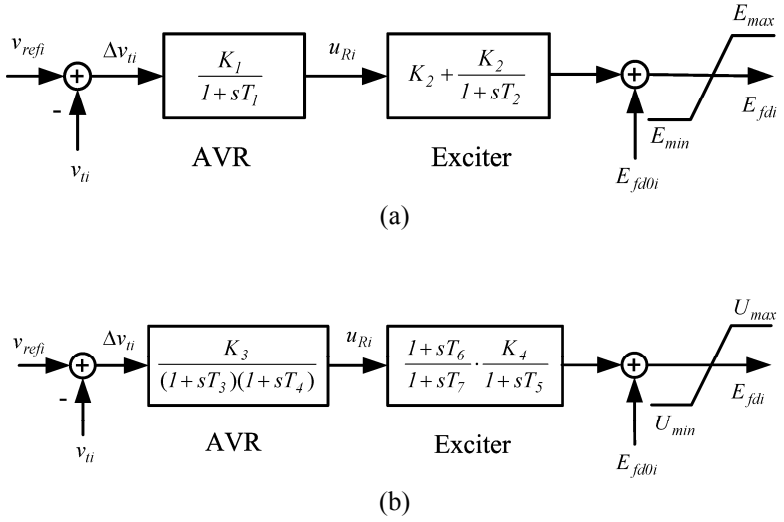

Fig. 6. Conventional excitation control system; a) for units 2 and 3, b) for units 1 and 4

Each unit has a full set of governor-turbine system (governor, steam valve servo-system, high-pressure turbine, intermediate-pressure turbine, and low-pressure turbine) which is shown in Fig. 7. The generators, lines, conventional excitation system and governor-turbine parameters are given in Table 1, Table 2, Table 3 and Table 4, respectively.

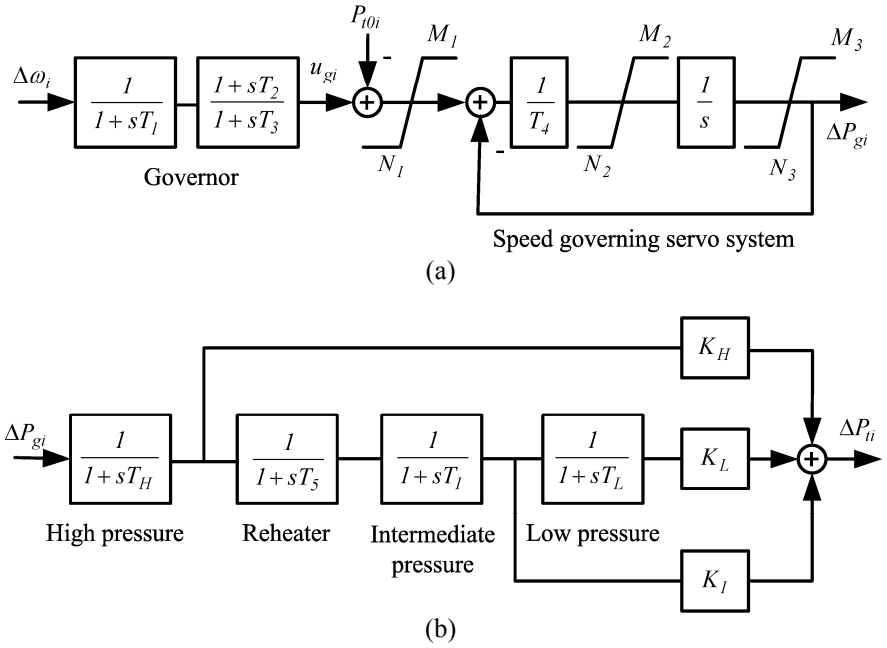

Fig. 7. a) Conventional speed governing system, b) Detailed turbine system

Table 1
Generator constants

Unit No.	M_i (*sec*)	D_i	x_{di} (*pu*)	x'_{di} (*pu*)	x_{qi} (*pu*)	x'_{qi} (*pu*)	T'_{d0i} (*sec*)	T'_{q0i} (*sec*)	MVA
1	8.05	0.002	1.860	0.440	1.350	1.340	0.733	0.0873	1000
2	7.00	0.002	1.490	0.252	0.822	0.821	1.500	0.1270	600
3	6.00	0.002	1.485	0.509	1.420	1.410	1.550	0.2675	1000
4	8.05	0.002	1.860	0.440	1.350	1.340	0.733	0.0873	900

Table 2
Line parameters

Line No.	*Bus-Bus*	R_{ij} (*pu*)	X_{ij} (*pu*)	S_{ij} (*pu*)
1	1-9	0.02700	0.1304	0.0000
2	2-10	0.07000	0.1701	0.0000
3	3-11	0.04400	0.1718	0.0000
4	4-12	0.02700	0.1288	0.0000
5	10-6	0.02700	0.2238	0.0000
6	11-7	0.04000	0.1718	0.0000
7	12-8	0.06130	0.2535	0.0000
8	9-10	0.01101	0.0829	0.0246
9	10-11	0.01101	0.0829	0.0246
10	11-12	0.01468	0.1105	0.0328
11	12-5	0.12480	0.9085	0.1640

Table 3
Excitation parameters

K_1	K_2	K_3	K_4	$\lvert E_{max(min)} \rvert$	U_{max}	U_{min}
1.00	19.21	10.00	6.48	5.71	7.60	-5.20
T_1	T_2	T_3	T_4	T_5	T_6	T_7
(*sec*)	(*sec*)	(*sec*)	(*sec*)	(*sec*)	(*sec*)	(*s*)
0.010	1.560	0.013	0.013	0.200	3.000	10.000

Table 4
Governor and turbine parameters

Parameters	Unit 1	Unit 2	Unit 3	Unit 4
T_1 (Sec)	0.08	0.06	0.07	0.07
T_2 (Sec)	0.10	0.10	0.10	0.10
T_3 (Sec)	0.10	0.10	0.10	0.10
T_4 (Sec)	0.40	0.36	0.42	0.42
T_5 (Sec)	10.0	10.0	10.0	10.0
T_H (Sec)	0.05	0.05	0.05	0.05
T_I (Sec)	0.08	0.08	0.08	0.08
T_L (Sec)	0.58	0.58	0.58	0.58
K_H (pu)	0.31	0.31	0.31	0.31
K_I (pu)	0.24	0.24	0.24	0.24
K_L (pu)	0.45	0.45	0.45	0.45
M_1 (pu/Minute)	0.50	0.50	0.50	0.50
M_2 (pu/Minute)	0.20	0.20	0.20	0.20
M_3 (pu/Minute)	1.50	1.50	1.50	1.50
N_1 (pu/Minute)	-0.50	-0.50	-0.50	-0.50
N_2 (pu/Minute)	-0.20	-0.20	-0.20	-0.20
N_3 (pu/Minute)	-0.50	-0.50	-0.50	-0.50

Unit 1 is selected to be equipped with robust control, and therefore our objective is to apply the control strategy described in the previous section to controller design for unit 1. The whole power system has been implemented in the mentioned laboratory. Fig. 8 shows the overview of the applied laboratory experiment devices including the control/monitoring desks. A digital oscilloscope and a notebook computer (shown in Fig. 8b) are used for monitoring purposes.

The proposed control loop (Fig. 9) has been built in a personal computer were connected to the power system using a digital signal processing (DSP) board equipped with analog to digital (A/D) and digital to analog (D/A) converters as the physical interfaces between the personal computer and the analog power system hardware. In Fig. 9, the input/output scaling blocks are used to match the PC based controller and the Analog Power System hardware, signally. High frequency noises are removed by appropriate low pass filters.

(a)

(b)

Fig. 8. Performed laboratory experiment; a) Overview of Analog Power System Simulator, b) the control/monitoring desks

Then, applying the proposed H∞-SOF control methodology an optimal gain vector for the problem at hand is obtained as follows.

$$K_{1,SOF} = \begin{bmatrix} 9.5899 & 7.8648 & 1.2990 \end{bmatrix} \tag{24}$$

Running the proposed algorithm for a pure optimal gain vector design (without conventional AVR-PSS) gives the following result:

$$K_{1,SOF} = \begin{bmatrix} 9.9897 & 8.9987 & 1.5986 \end{bmatrix} \tag{25}$$

The considered constraints on limiters and control loop gains are set according to the real power system control units and close to ones that exist for the conventional AVR_PSS units. The used constant weight vector (η_i) is given in Appendix.

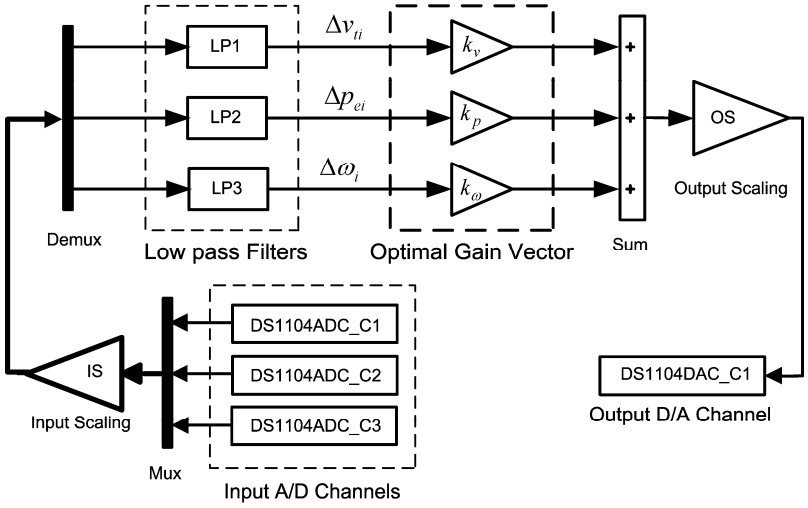

Fig. 9. The performed computer based control loop

4. Experiment Results for OGV Design in the Presence of Conventional AVR-PSS

The performance of the closed-loop system using the proposed optimal gain vector (OGV) in comparison of a pure conventional AVR-PSS system is tested in the presence of voltage deviation, faults and system disturbance. The configuration of the applied conventional power system stabilizer, which was accurately tuned by the system operators, is illustrated in Fig. 10. The conventional PSS parameters are listed in table 5.

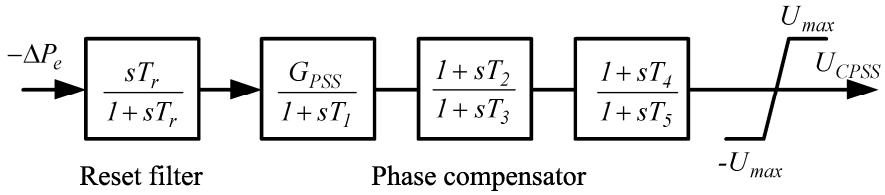

Fig. 10. Conventional power system stabilizer

Table 5
Conventional PSS parameters

T_r (*sec*)	G_{PSS}	U_{max} (*pu*)	T_1 (*sec*)
5.00	10.00	1.00	0.025
T_2 (*sec*)	T_3 (*sec*)	T_4 (*sec*)	T_5 (*sec*)
0.056	0.054	0.037	0.53

During the first test scenario, the output setting of unit 1 is fixed to 0.5 pu. Fig. 11 shows the electrical power, terminal voltage and machine speed of unit 1, following a fault on the line between buses 11 and 12 at 2 *sec*. It can be seen that the system response is quite improved using the designed feedback gains.

Furthermore, the size of resulted stable region by the proposed method is significantly enlarged in comparison of conventional AVR-PSS controller. To show this fact, the critical power output from unit 1 in the presence of a three-phase to ground fault is considered as a good measure. To investigate the critical point, the real power output of unit 1 is increased from 0.3 pu (The setting of the real power output from the other units is fixed at the values shown in Fig. 5). Using the conventional AVR-PSS structure, the resulted critical power output from unit 1 to be 0.31 pu; and in case of tight tuning of CPSS parameters it could not be higher than 0.52 pu. For the proposed control method, the critical power output, as shown in Table 6, is increased to 0.94 pu.

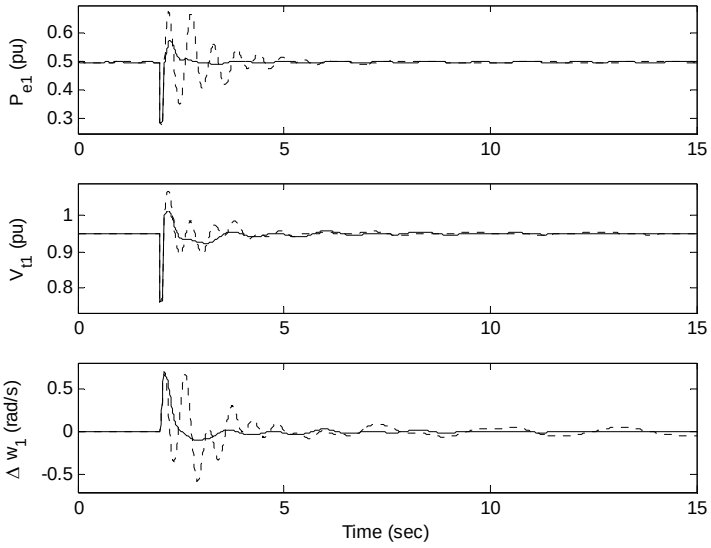

Fig. 11. System response for a fault between buses 11 and 12; Solid (Using OGV), dotted (Conventional AVR-PSS)

Table 6
Critical power output of Unit 1

Control design	*Critical power output*
Proposed design	*0.94* (*pu*)
Conventional AVR-PSS	*0.52* (*pu*)

The system response for a fault between buses 11 and 12, while the output setting of unit 1 is increased to 0.7 pu is shown in Fig. 12. In the second test case, the performance of designed controllers was evaluated in the presence of a 0.05 pu step disturbance injected at the voltage reference input of unit 1 at 20 *sec*.

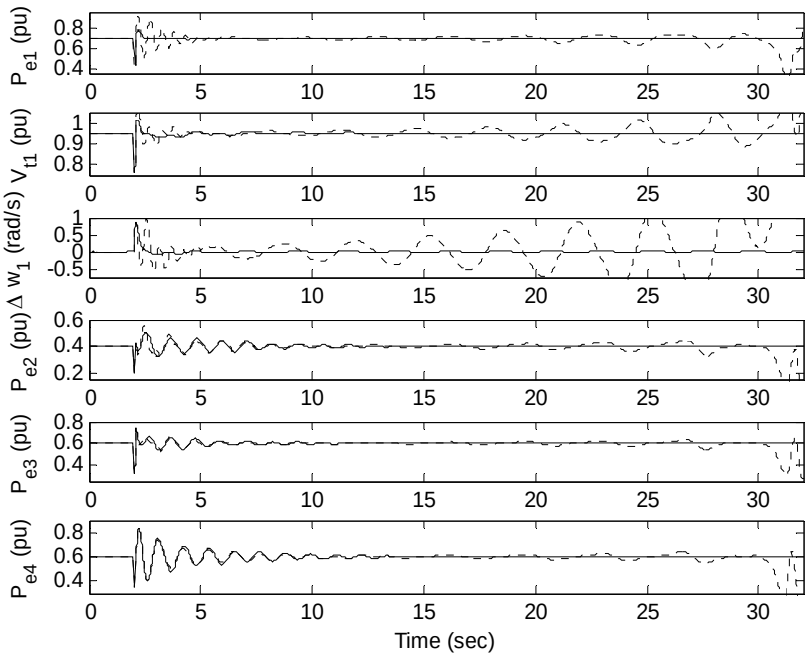

Fig. 12. System response for a fault between buses 11 and 12, while the output setting of unit 1 is fixed to 0.5 pu.; Solid (Using OGV), dotted (Conventional AVR-PSS)

Fig. 13 shows the closed-loop response of the power systems fitted with the conventional control and the proposed robust control design. The better performance is achieved by the developed control strategy.

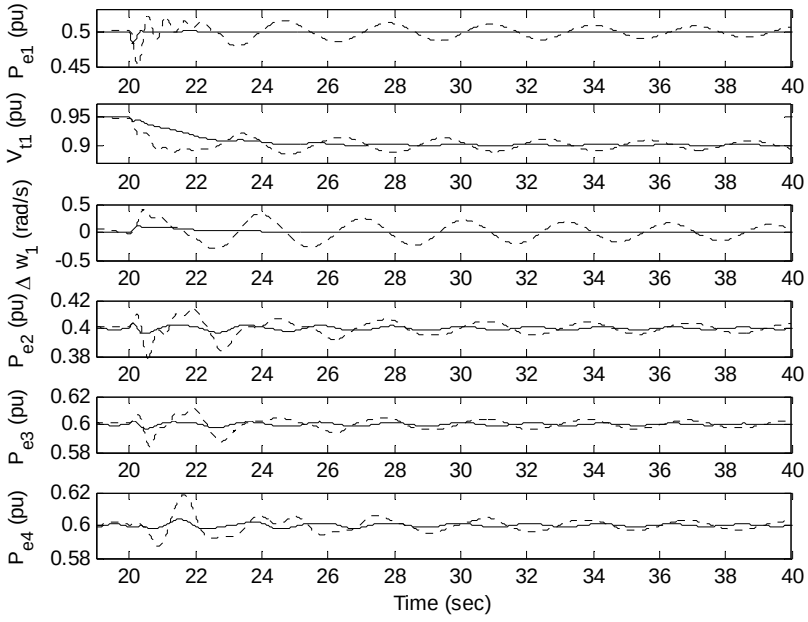

Fig. 13. System response for a 0.05 pu step change at the voltage reference input of unit 1; Solid (Using OGV), dotted (Conventional AVR-PSS)

Finally, the system response in the face of a step disturbance (d_i) in the closed-loop system at 20 *sec*, is shown in Fig. 14. Comparing the experiment results shows that the robust design achieves robustness against the voltage deviation, disturbance and line fault with a quite good voltage regulation and damping performance.

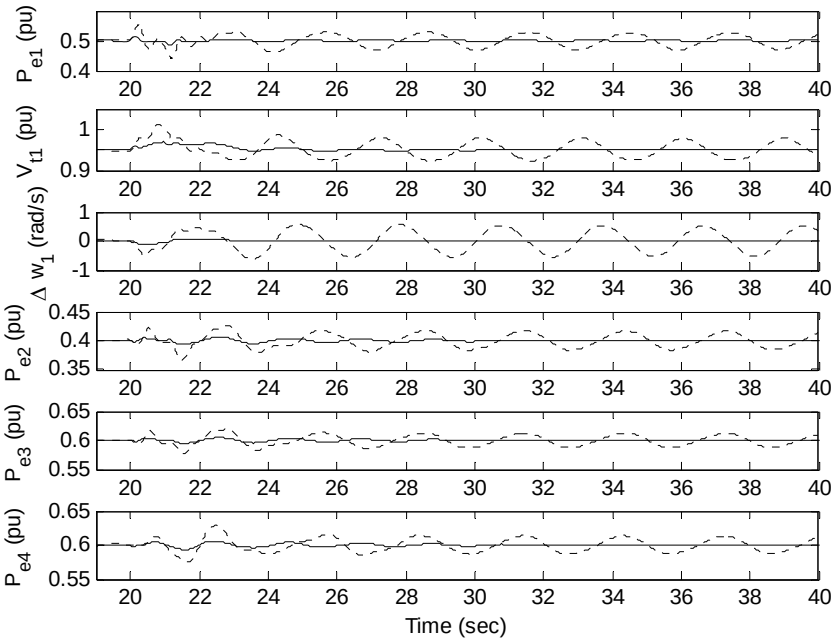

Fig. 14. System response for a step disturbance at 20 *sec*; Solid (Using OGV), dotted (Conventional AVR-PSS)

5. Experiment Results for the Pure OGV Design

In the next step, a designed pure OGV is applied to the power system shown in Fig. 5. Here, the performance of the closed-loop system in comparison of a full-order dynamic H∞ output feedback controller is tested in the presence of voltage deviation, faults and system disturbance. During the real-time nonlinear experiments, the output setting of unit 1 is fixed to 0.6 pu.

Fig. 15 shows the electrical power, terminal voltage and machine speed of unit 1, and the electrical powers of other units, following a fault on the line between buses 11 and 12 at 2 *sec*. The fault is continued for 4 cycles. As the next test case, the performance of designed controllers was evaluated in the presence of a 0.05 pu step disturbance injected at the voltage reference input of unit 1 at 20 *sec*. Fig. 16 shows the closed-loop response of the power systems fitted with the dynamical H∞ controller and the proposed robust gain vector.

System response in the face of a step disturbance (d_i) with one second duration in the closed-loop system at 20 *sec*, is shown in Fig. 17. Comparing the experiment results shows that the robust design achieves robustness against the voltage deviation, disturbance and line fault with a quite good performance as well as full dynamical H∞ controller. Furthermore, practically it is highly desirable,

for reasons of simplicity of structure and flexibility of design methodology.

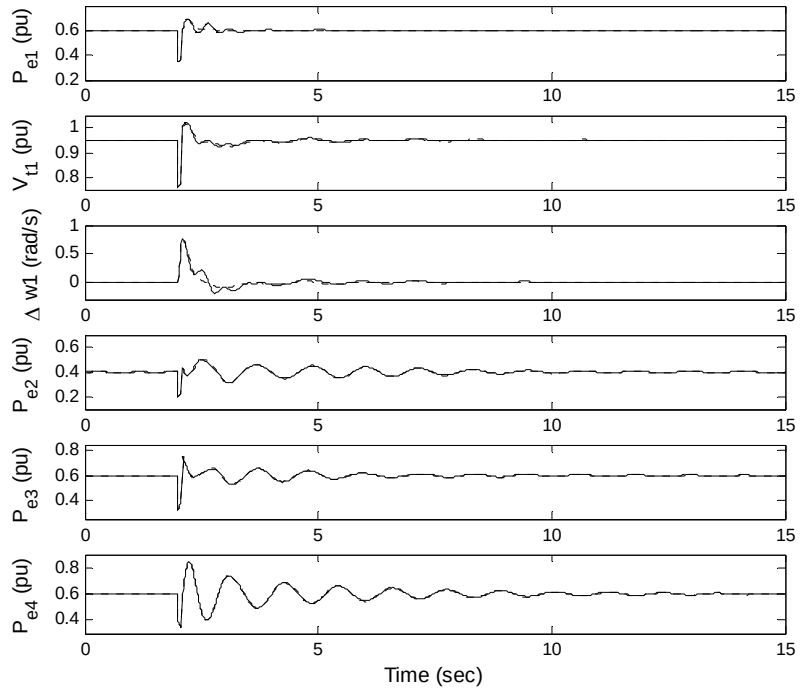

Fig. 15. System response for a fault between buses 11 and 12; Solid (H∞-SOF), dotted (H∞-Dynamic)

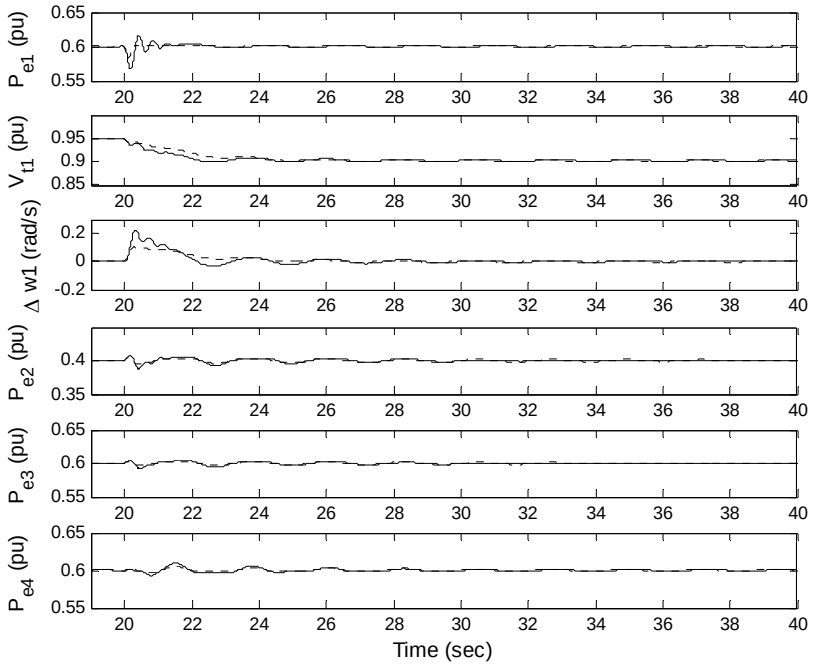

Fig. 16. System response for a 0.05 pu step change at the voltage reference input of unit 1; Solid (H∞-SOF), dotted (H∞-Dynamic)

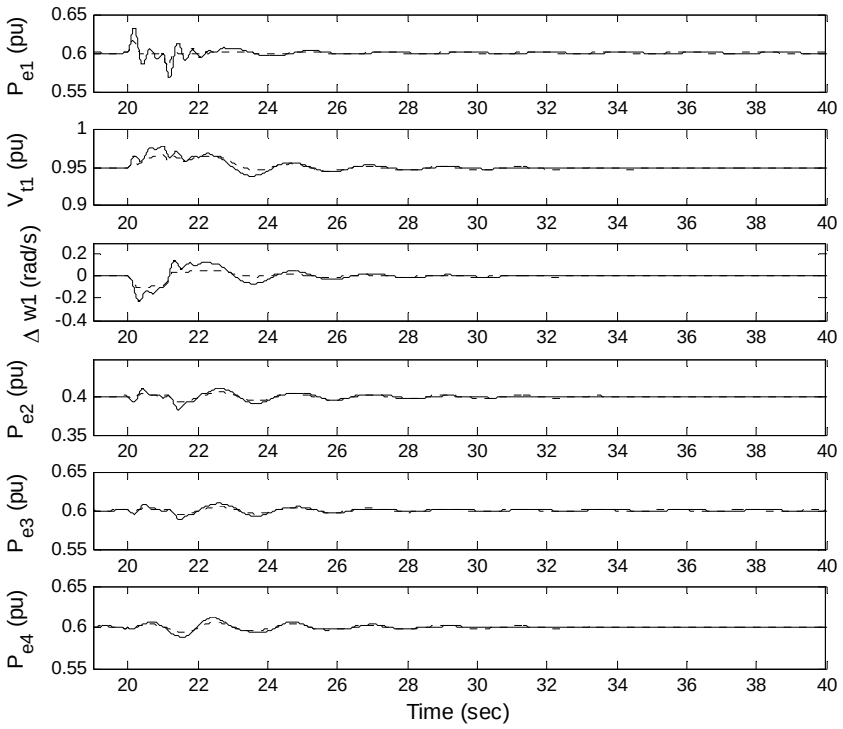

Fig. 17. System response for a step disturbance at 20 *sec*; Solid (H∞-SOF), dotted (H∞-Dynamic)

Table 7 shows a comparison between the proposed H∞-SOF and H∞-Dynamic approaches in view point of structure, robust performance indices and the critical power output from unit 1 for a three-phase to ground fault (between buses 11 and 12 in Fig. 5). To investigate the critical point, the real power output of unit 1 is increased from 0.1 pu (The setting of the real power output from the other units is fixed at the values shown in Fig. 5).

The size of resulted stable region by both methods is approximately equal, and it is significantly enlarged in comparison of conventional AVR-PSS controller. Using the conventional AVR-PSS structure, the resulted critical power output from unit 1 to be 0.31 pu; and in case of tight tuning of parameters it will not to be higher than 0.5 pu.

Table 7
Comparison of H∞-based proposed robust control designs

Control design	*Control structure*	*Robust Perf. index*	*Critical power output*
H∞-Dynamic	High order	$\gamma = 455.1052$	*0.95* (*pu*)
H∞-SOF	Pure gain	$\gamma^* = 456.3110$	*0.93* (*pu*)
AVR-PSS	Conventional	-	*0.50* (*pu*)

Finally, to demonstrate the simultaneous damping of local (fast) and global (slow) oscillation modes, filtering analysis has been performed. For the study system, the local mode for each

corresponding unit, and the low frequency global mode are around 1.5 Hz and 0.3 Hz, respectively. The laboratory results for the speed deviation of unit 1, following a fault on the line between buses 11 and 12 are shown in Fig. 18. The results are compared with a tight-tuned conventional AVR-PSS type (Hiyama, Kawakita & Ono, 2004) in a stable operating condition.

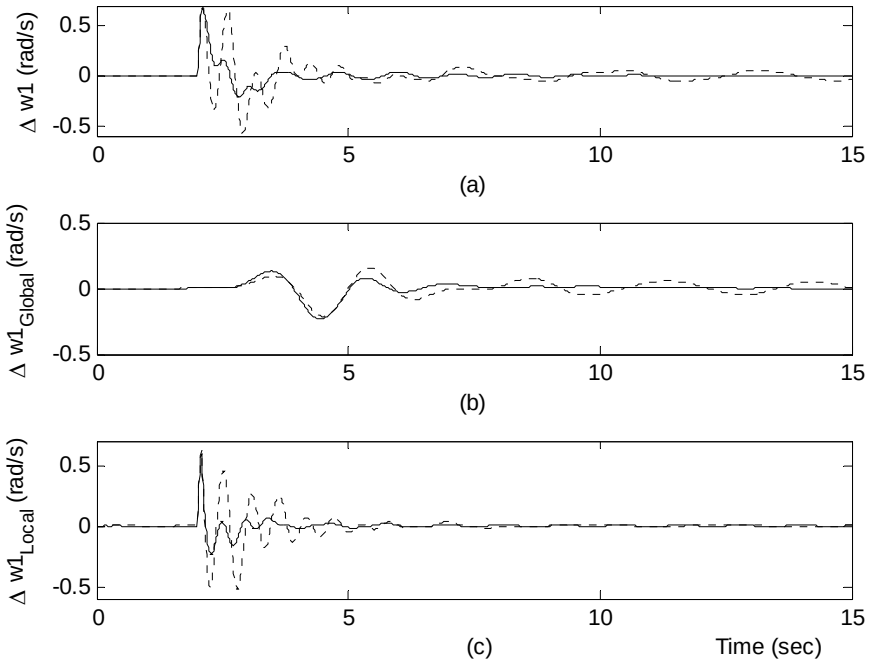

Fig. 18. Oscillation modes analysis, following a fault; a) Speed deviation, b) Global mode, c) fast mode. Solid (H∞-SOF), dotted (Conventional AVR-PSS by Hiyama, Kawakita & Ono, 2004)

6. Conclusion

In order to simultaneous enhancement of power system stability and voltage regulation, a new control strategy is developed using an H∞-SOF control technique via a developed iterative LMI algorithm. The proposed method was applied to a four-machine infinite bus power system, through a laboratory real-time experiment, and the results are compared with a conventional AVR-PSS and dynamic H∞ control designs. The performance of the resulting closed-loop system is shown to be satisfactory over a wide range of operating conditions.

As shown in the nonlinear real-time simulation results, the proposed coordination through a new optimal feedback loop has brought a significant effect to improve the power system performance and to widen the stable region. The resulting controller is not only robust but it also allows direct effective trade-off between voltage regulation and damping performance. Furthermore, because of simplicity of structure, decentralized property, ease of formulation and flexibility of design methodology, it is practically desirable.

Appendix

The elements of A_{gi} matrix in (11):

$$a_{21} = -\frac{1}{M_i}\frac{\partial f_{1i}(x)}{\partial x_{1gi}}\bigg|_{x_{egi}}$$

$$a_{23} = -\frac{\left[G_{ii}E'^{e}_{qi} - B_{ii}E'^{e}_{di} + I^{e}_{qi}\right]}{M_i} - \frac{1}{M_i}\frac{\partial f_{1i}(x)}{\partial x_{3gi}}\bigg|_{x_{egi}}$$

$$a_{24} = -\frac{\left[G_{ii}E'^{e}_{di} + B_{ii}E'^{e}_{qi} + I^{e}_{di}\right]}{M_i} - \frac{1}{M_i}\frac{\partial f_{1i}(x)}{\partial x_{4gi}}\bigg|_{x_{egi}}$$

$$a_{31} = -\frac{\Delta x_{di}}{T'_{d0i}}\frac{\partial f_{2i}(x)}{\partial x_{1gi}}\bigg|_{x_{egi}}, \; a_{33} = -\frac{1}{T'_{d0i}} + \frac{B_{ii}\Delta x_{di}}{T'_{d0i}}$$

$$a_{41} = -\frac{\Delta x_{qi}}{T'_{q0i}}\frac{\partial f_{3i}(x)}{\partial x_{1gi}}\bigg|_{x_{egi}}, \; a_{44} = -\frac{1}{T'_{q0i}} + \frac{B_{ii}\Delta x_{qi}}{T'_{q0i}}$$

where

$$f_{1i}(x) = x_{4gi}\Delta I_{di}(x) + x_{3gi}\Delta I_{qi}(x) + \sum_{k\neq i}\Big\{[E'^{e}_{di}\eta_{ik}(\delta) + E'^{e}_{qi}\hat{\eta}_{ik}(\delta)]x_{4gk}$$
$$+[E'^{e}_{di}\nu_{ik}(\delta) + E'^{e}_{qi}\hat{\nu}_{ik}(\delta)]x_{3gk} + [E'^{e}_{di}\upsilon_{ik}(\delta) + E'^{e}_{qi}\hat{\upsilon}_{ik}(\delta)]\sin\phi_{ik}\Big\}$$

$$f_{2i}(x) = \sum_{k\neq i}\left[\eta_{ik}(\delta)x_{4gk} + \nu_{ik}(\delta)x_{3gk} + \upsilon_{ik}(\delta)\sin\phi_{ik}\right]$$

$$f_{3i}(x) = \sum_{k\neq i}\left[\hat{\eta}_{ik}(\delta)x_{4gk} + \hat{\nu}_{ik}(\delta)x_{3gk} + \hat{\upsilon}_{ik}(\delta)\sin\phi_{ik}\right]$$

$$\eta_{ik}(\delta) = G_{ik}\cos\delta_{ik} + B_{ik}\sin\delta_{ik}, \; \hat{\eta}_{ik}(\delta) = B_{ik}\cos\delta_{ik} - G_{ik}\sin\delta_{ik}$$

$$\nu_{ik}(\delta) = G_{ik}\sin\delta_{ik} - B_{ik}\cos\delta_{ik}, \; \hat{\nu}_{ik}(\delta) = B_{ik}\sin\delta_{ik} - G_{ik}\cos\delta_{ik}$$

$$\upsilon_{ik}(\delta) = 2gI_{ik}\sin\frac{\delta^{e}_{ik} + \delta_{ik}}{2} + 2g2_{ik}\cos\frac{\delta^{e}_{ik} + \delta_{ik}}{2}, \; \phi_{ik} = 0.5(x_{1gi} - x_{1gk})$$

$$\hat{\upsilon}_{ik}(\delta) = 2g2_{ik}\sin\frac{\delta^e_{ik}+\delta_{ik}}{2} - 2gI_{ik}\cos\frac{\delta^e_{ik}+\delta_{ik}}{2},\ \ \delta_{ik} = \delta_i - \delta_k$$

$$gI_{ik} = G_{ik}E'^e_{dk} - B_{ik}E'^e_{qk},\ \ g2_{ik} = G_{ik}E'^e_{qk} + B_{ik}E'^e_{qk}$$

Constant weights: $\eta_1 = [0.25 \quad 0.1 \quad 5]$

References

Bevrani, H., & Hiyama, T. (2006). Stability and voltage regulation enhancement using an optimal gain vector. Proc. of *IEEE PES General Meeting*, Canada.

Boyd, S. P., El Chaoui, L., Feron, E., & Balakrishnan, V. (1994). Linear matrix inequalities in systems and control theory. Philadelphia, PA: SIAMA.

Cao, Y. Y, Lam, J., Sun, Y. X., & Mao, W. J. (1998). Static output feedback stabilization: an ILMI approach. *Automatica*, 34(12), 1641-1645.

Guo, Y., Hill, D. J., & Wang, Y. (2001). Global transient stability and voltage regulation for power systems. *IEEE Trans on Power Systems,* 16(4), 678-688.

Heniche, A., Bourles, H., & Houry, M. P. (1995). A desensitized controller for voltage regulation of power systems. *IEEE Trans on Power Systems,* 10(3), 1461-1466.

Hiyama, T., Oniki, S., &. Nagashima, H. (1996). Evaluation of advanced fuzzy logic PSS on analog network simulator and actual installation on hydro generators. *IEEE Trans on Energy Conversion*. 11(1), 125-131.

Hiyama, T., Kawakita, M., & Ono, H. (2004). Multi-agent based wide area stabilization control of power systems using power system stabilizer. Proc. of *IEEE Int Conf on Power System Technology*.

Hiyama, T., Kojima, D., Ohtsu, K., & Furukawa, K. (2005). Eigenvalue-based wide area stability monitoring of power systems. *Control Engineering Practice.* 13, 1515-1523.

Kundur, P., Paserba, J., Ajjarapu, V., Andersson, G., Bose, A., Canizares, C., Hatziargyriou, N., Hill, D., Stankovic, A., Taylor, C., Cutsem T. V., & and Vittal, V. (200 4).Definition and classification of power system stability. *IEEE Trans on Power Systems,* 19(2), 1387-1401.

Law, K. T., Hill, D. J., & Godfrey, N. R. (1994). Robust co-ordinated AVR-PSS design. *IEEE Trans on Power Systems,* 9(3), 1218-1225.

Law, K. T., Hill, D. J., & Godfrey, N. R. (1994). Robust controller structure for coordinated power system voltage regulator and stabilizer design. *IEEE Trans on Control Systems Technology,* 2(3), 220-232.

Malik, O. P., Hope, G. S., Gorski, Y. M., Uskakov, V. A., & Rackevich, A. L. (1986). Experimental studies on adaptive microprocessor stabilizers for synchronous generators. *IFAC Power System and Power Plant Control*, Beijing, China, 125-130.

Sauer, P. W., & Pai, M. A. (1998). Power system dynamic and stability. Englewood Cliffs, NJ; Prentice-Hall.

Soliman, H. M., & Sakar, M. M. F. (1988). Wide-range power system pole placer. *Inst Elect Eng Proc*, Part C, 135(3), 195-200.

Venikov, V. A., & Stroev, V. A. (1971). Power system stability as affected by automatic control of generators-some methods of analysis and synthesis. *IEEE Trans PAS,* PAS-90, 2483-2487.

Wang, Y. & Hill, D. J. (2001). Robust nonlinear coordinated control of power systems. *Automatica*, 32(4), 611-618.

Yadaiah, N., Kumar, A. G. D., & Bhattacharya, J. L. (2004). Fuzzy based coordinated controller for power system stability and voltage regulation. *Electric Power System Research*, 69, 169-177.

چکیده

بطـور معمـول، طراحـی تنظـیم‌کننـده خودکـار ولتـاژ (Automatic Voltage Regulator-AVR) و پایدارساز دینامیکی سیستم قدرت (Power System Stabilizer-PSS) بصورت دو طراحـی مجـزا و در دو مرحله جداگانه صورت می‌پذیرد. ابتدا AVR جهت دست‌یابی به شاخص‌های مناسـب ولتـاژی طراحـی و اجـرا می‌شود و سپس PSS برای برآوردن نیازهای پایداری و میرایی مطلوب نوسانات در شبکه طراحی می‌گردد.

اکنون بخوبی مشخص شده است که عملکرد AVR وPSS دارای تداخل ذاتی بوده و بهبود عملکرد یکـی، کیفیت عملکرد دومی را تحت‌تاثیر قرارمی‌دهد بطوریکه طراحی مستقل و متوالی آنها نمی‌تواند شرایط لازم بـرای تحقق عملکرد بهینه را در هر دو راستای تنظیم ولتاژ و میرایی نوسانات فراهم‌آورد. بنابرایـن تـلاش بـرای تحقـق اهداف ذکرشده با طراحی همزمان AVR وPSS در یک ساختار کنترل واحد منطقی به نظرمی‌رسد.

در این تحقیق، یک روش جدید کنترل مقاوم و در حین‌حال ساده جهت بهبود همزمان پایداری و تنظیم ولتاژ سیستمهای قدرت ارایه شده‌است. براساس این روش، ابتدا دو مسئله فوق در قالب یک مسئله واحد کنترل فیدبک استاتیک خروجی بیان و سپس برای حل آن، الگوریتمی مبتنی بر نامعادلات ماتریسی خطی(LMI) معرفی‌گردیـد. درستی الگوریتم طراحی حاصل از این تحقیق ابتدا توسط شبیه سازیهای کامپیوتری بررسی و سپس در آزمایشگاه مجهز Kyushu Electric Power Company در کشور ژاپن مورد آزمایش قرارگرفت. نتایج بدسـت‌آمـده، کارکرد مطلوب و رفتار مقاوم سیستم کنترل طراحی‌شده را نشان می‌دهند.

واژه های کلیدی:

تنظیم‌کننده خودکار ولتاژ(AVR)، پایدارساز دینامیکی (PSS)، کنترل مقـاوم، عملکـرد بهینـه، نامعـادلات ماتریسی خطی